



Effect of a siliceous additive on aqueous alteration of waste glass with engineered barrier materials

S. Mitsui^{a,*}, R. Aoki^b

^a Waste Isolation Research Division, Japan Nuclear Cycle Development Institute, 4-33 Tokai-mura, Naka-gun, Ibaraki 319-1194, Japan

^b Nuclear Energy System Inc., Tokai-mura, Naka-gun, Ibaraki 319-1194, Japan

Abstract

A simulated waste glass was leached in the presence of bentonite, iron and magnetite (as a corrosion product), with and without amorphous silica at 60°C for 364 days. These experiments were carried out to assess the effect of silica on the aqueous alteration of waste glass in contact with engineered barrier materials. The weight losses of samples without amorphous silica increased with time, while the weights of samples with amorphous silica were almost unchanged. This shows that the concentration of silicic acid in the porewaters reached the solubility of amorphous silica quickly, so that the detrimental effects of the engineered barrier materials were efficiently reduced. We also conducted MCC-1 type experiments with the same glass using silica saturated solutions at 60°C, 75°C and 90°C to understand the alteration mechanisms of glass under these conditions. The results show that the glass alteration under these conditions is dominated by glass hydration, and the release of soluble elements from the waste glass closely follows a relationship dependent on the square root of time. © 2001 Elsevier Science B.V. All rights reserved.

1. Introduction

As shown in Fig. 1, the Japanese engineered barrier system (EBS) for high level nuclear waste consists of vitrified waste, overpack and buffer material. Although the overpack and the buffer material are designed to prevent the release of radionuclides from the vitrified waste, some experiments have shown that these components and corrosion products of the overpack can promote glass dissolution. McVay and Buckwalter [1], Shade et al. [2] and McGrail [3] revealed that carbon steel, one of the candidates for the overpack material in Japan, increased the glass dissolution rate under oxidizing conditions. In the case of a large amount of iron, the dissolution rate increases by a factor of 20 compared with that of glass in deionized water. This detrimental effect of iron has been attributed to the formation of iron silicates. However, Imakita et al. [4] conducted glass dissolution experiments with carbon steel under reducing conditions, and noted that the effect of iron is neg-

ligible under reducing conditions. Inagaki et al. [5] performed glass dissolution experiments with magnetite, which is expected to be the major corrosion product of carbon steel overpack under reducing conditions, and showed that the presence of magnetite can enhance glass dissolution under those conditions. They suggested that precipitation of silica on the magnetite surface might be the dominant process for the enhancement. Godon et al. [6] investigated the dissolution behavior of waste glass in contact with several kinds of clays. They found that most clays act as silica sink, consuming silica released from the glass, and prevent the increase in Si concentration to saturation conditions, except for highly siliceous clay.

As described above, the detrimental effects of the engineered barrier materials on glass dissolution are related to the consumption of Si from solution. This implies that we can depress the detrimental effects by incorporating soluble siliceous material in the EBS. Godon et al. [7] demonstrated experimentally the effectiveness of silica additives in the presence of clay. Minet and Vernaz [8] calculated the long-term durability of the siliceous additives under repository conditions, and concluded that a few kilograms of silica additives can considerably enhance the waste glass durability.

* Corresponding author. Tel.: +81-29 287 3642; fax: +81-29 287 3704.

E-mail address: natural@tokai.jnc.go.jp (S. Mitsui).

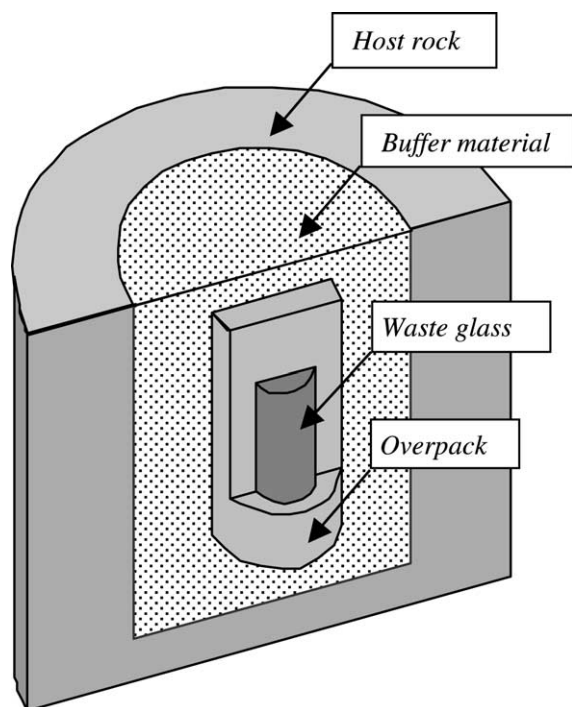


Fig. 1. The basic concept of geological disposal in Japan.

This study was conducted to assess the effect of silica on the aqueous alteration of waste glass in contact with engineered barrier materials. A simulated waste glass (P0798) was leached in the presence of bentonite, iron and magnetite (as a corrosion product of carbon steel overpack), with and without a siliceous additive (amorphous silica). MCC-1 type static leaching experiments with P0798 glass using silica saturated solutions were also conducted to understand the alteration mechanisms of glass under the conditions affected by the siliceous additive.

2. Experimental methods

2.1. Glass sample

A simulated waste glass P0798, developed by Japan Nuclear Cycle Development Institute (JNC), was used as a specimen. The composition of P0798 is shown in Table 1. Samples with dimensions of 10 mm × 10 mm × 1 mm were finely polished (with cerium oxide for the final polish) on all the surfaces. The samples were cleaned ultrasonically with ethanol, and the weight of the samples was measured before use.

2.2. Integrated leaching experiments

The integrated leaching experiments in the presence of engineered barrier materials were performed in

Table 1
Composition of P0798 glass

Oxide	wt%	Oxide	wt%
SiO ₂	46.60	MnO ₂	0.37
Al ₂ O ₃	5.00	RuO ₂	0.74
Fe ₂ O ₃	2.04	Rh ₂ O ₃	0.14
CaO	3.00	PdO	0.35
Na ₂ O	10.00	Ag ₂ O	0.02
B ₂ O ₃	14.20	CdO	0.02
Li ₂ O	3.00	SnO ₂	0.02
ZnO	3.00	SeO ₂	0.02
P ₂ O ₅	0.30	TeO ₂	0.19
Cr ₂ O ₃	0.10	Y ₂ O ₃	0.18
NiO	0.23	La ₂ O ₃	0.42
Rb ₂ O	0.11	CeO ₂	3.34
Cs ₂ O	0.75	Pr ₈ O ₁₁	0.42
SrO	0.30	Nd ₂ O ₃	1.38
BaO	0.49	Sm ₂ O ₃	0.29
ZrO ₂	1.46	Eu ₂ O ₃	0.05
MoO ₃	1.45	Gd ₂ O ₃	0.02

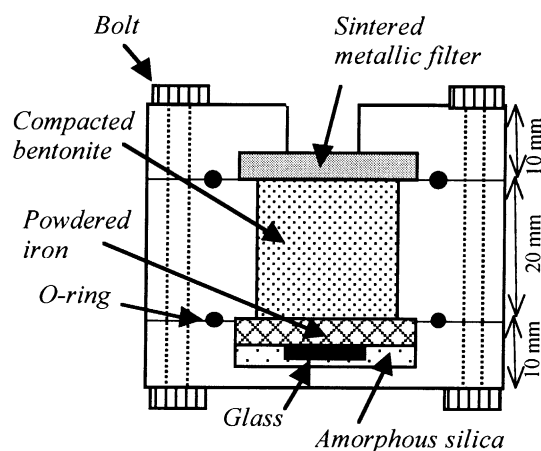


Fig. 2. Leaching vessel for the integrated leaching experiments. This figure shows a combination of glass/silica/iron as an example. The combinations of the materials in the bottom part were glass/bentonite, glass/magnetite, glass/iron, glass/silica and glass/silica/iron. Each vessel contains compacted bentonite in the middle part.

polycarbonate leaching vessels (Fig. 2). The vessel consists of three parts in order to simulate the Japanese EBS. The bottom part of the leaching vessels contains the glass sample and engineered barrier material (bentonite, iron powder or magnetite powder) with and without amorphous silica powder in five different combinations. The combinations were glass/bentonite, glass/magnetite, glass/iron, glass/amorphous silica and glass/amorphous silica/iron. The middle part encloses a compacted sodium bentonite. The sodium bentonite used is Kunigel V1[®] (for the mineralogy of Kunigel V1[®] see [9]) from Kunimine Industries. The cavity containing

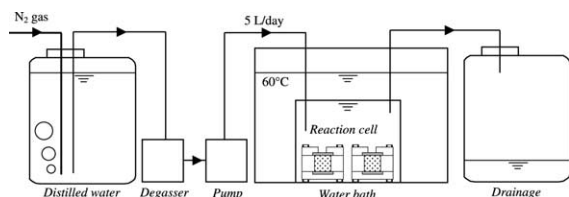


Fig. 3. Schematic view of the integrated leaching experiment apparatus.

bentonite was filled so that the dry powder has a dry density of 1.0 g/cm^3 . The bentonite was then saturated with distilled water and the bottom part was attached. On the top of the vessels, a stainless steel sintered filter was placed to permit exchange of water. After assembly, the vessels were immersed in distilled water in Teflon-coated reaction cells which were kept at 60°C by using a water bath (Fig. 3). The distilled water was purged with N_2 gas and was replaced continuously with a high pressure liquid chromatography (HPLC) pump at a flow rate of approximately 5 l/day. A degasser was placed between the distilled water reservoir and the pump to avoid bubble formation. The integrated leaching experiments were carried out for 28, 56, 91, 182 and 364 days. After each experimental period, the weight losses of the glass samples were measured. The glass alteration layer of some selected samples was analyzed by secondary ion mass spectrometry (SIMS).

2.3. MCC-1 type leaching experiments in silica saturated solutions

We also performed MCC-1 type experiments [10] using the same shape glass specimens and silica saturated solutions. The silica saturated solutions were prepared by dissolving amorphous silica (Soekawa Chemical; purity 99.99%) in distilled water at 60°C , 75°C and 90°C for 1 month. Analyses of the solutions using inductively coupled plasma atomic emission spectrometry (ICP-AES) showed Si concentrations of 84, 110 and 150 g/m^3 at 60°C , 75°C and 90°C , respectively. The ratio of surface area to solution volume (SA/V) was 10 m^{-1} . As in the first series of experiments, we leached the glass specimen at 90°C for a period of 400 days to understand the long-term glass alteration. In the second series of experiments, we investigated the effects of temperature on the alteration rate. Samples were leached at 60°C and 75°C for 100 days. After the leaching experiments, the glass samples were subjected to several surface analyses, including optical microscopy (OM), SIMS, transmission electron microscopy (TEM) with Energy dispersive X-ray spectrometry (EDS), and X-ray diffraction (XRD) with a thin film attachment which can be used for XRD analysis of a very thin layer ($>10 \text{ nm}$ thick). The solution was analyzed for several

components of the glass using ICP-AES and atomic absorption spectrometry (AAS).

3. Results and discussions

3.1. Integrated leaching experiments

The weight losses and the dissolution rates of samples as a function of time are shown in Figs. 4 and 5,

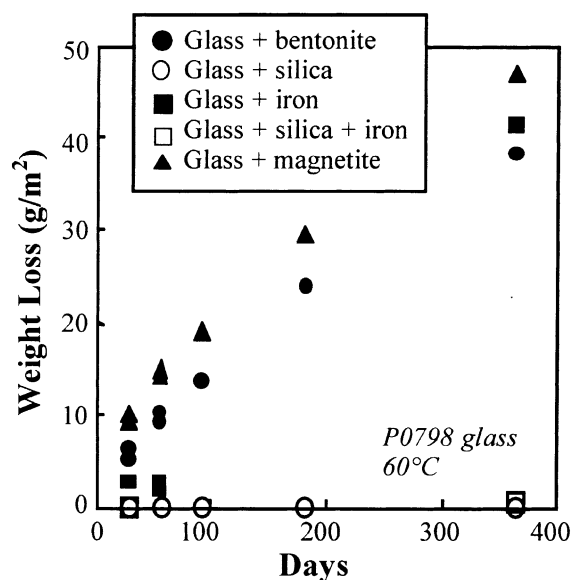


Fig. 4. Weight losses versus time.

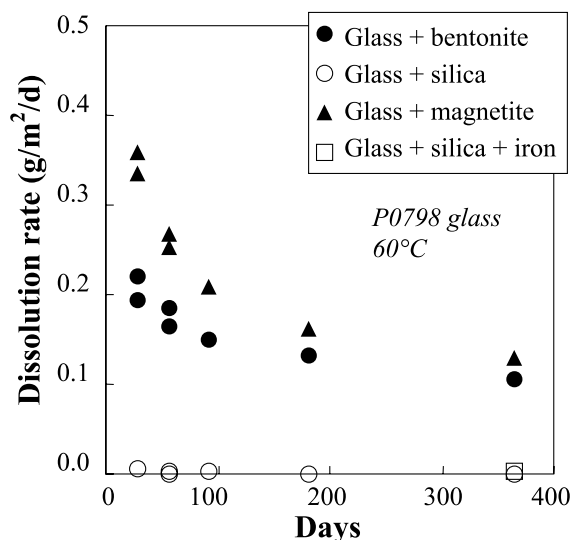


Fig. 5. Dissolution rates versus time.

respectively. The values for the glass/iron combination may be underestimated because small amount of iron particles adhere to the samples. The weight losses of samples without amorphous silica increased with time,

while those of samples with amorphous silica were almost unchanged. This agrees with the results of Godon et al. [6]. The dissolution rates based on weight loss for the combination of glass/bentonite and glass/magnetite

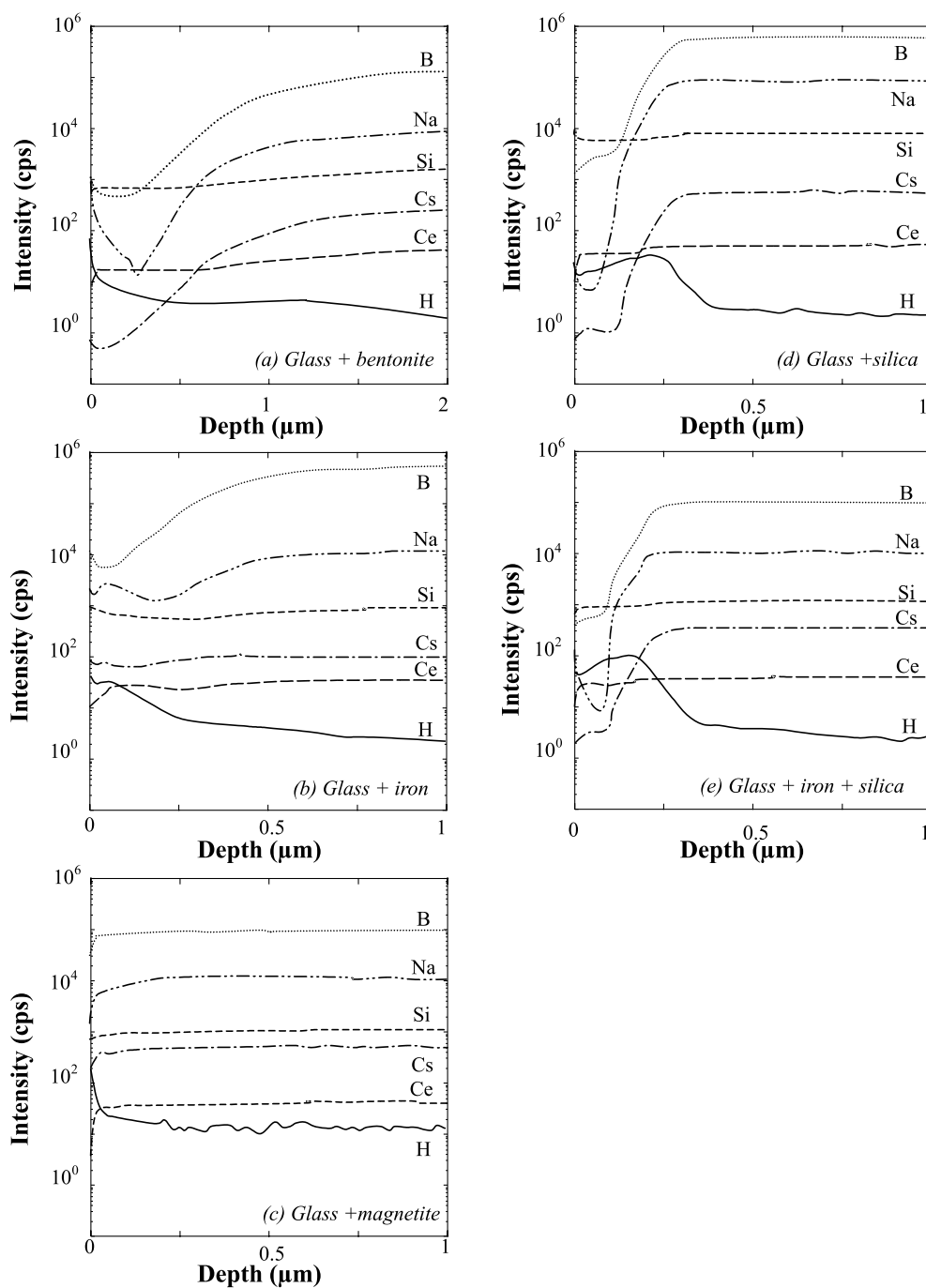


Fig. 6. SIMS depth profiles for P0798 glass after 182 days leaching with engineered barrier materials at 60°C. (All profiles are normalized to that of the 'inert' element Al.)

were around $0.1 \text{ g/m}^2/\text{day}$ after 364 days. On the other hand, the dissolution rates for the combinations glass/silica and glass/silica/iron were very low, on the order of 10^{-3} or $10^{-4} \text{ g/m}^2/\text{day}$. These results indicate that the concentration of silicic acid in the porewaters reached the solubility of amorphous silica quickly, so that the detrimental effects of the engineered barrier materials were efficiently reduced.

Fig. 6 shows SIMS profiles of H, B, Na, Cs, Ce and Si for the samples leached for 182 days. Although the other samples have altered layers, the sample for the combination of glass/magnetite has no altered layer. This result indicates that glass dissolution for this combination is congruent, whereas those for the others are selective.

3.2. MCC-1 type leaching experiments in silica saturated solutions

The surfaces of glass samples after leaching were glossy and showed no visible alteration. However, optical microscope and transmission electron microscope observations exhibited an altered layer on the surface of the sample leached at 90°C for 400 days. Fig. 7 is a photomicrograph of a thin section of the sample. In this figure, an altered layer was observed. The position of the altered surface is the same as that of the original surface, which is indicated by the polished surface of the opaque particle located in the center of the figure. This observation implies that matrix dissolution is negligible under silica saturation conditions. Fig. 8 shows TEM photomicrographs of the same sample. Some fracturing of the glass has occurred during the microtomy due to differences in the hardness of the glass and epoxy resin. It can be seen that the $4 \mu\text{m}$ thick altered layer (Fig. 8(a)), that is slightly lighter than the unaltered glass, is not composed of a porous ‘gel’ as formed by matrix dissolution. Analysis of the altered layer with EDS shows depletion

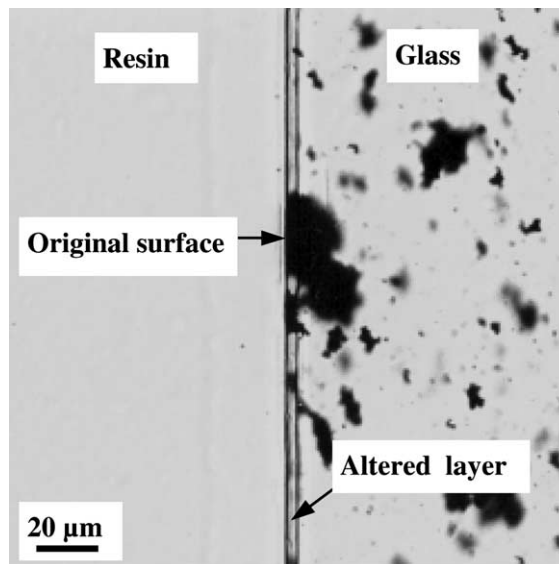


Fig. 7. Photomicrograph of a thin section of P0798 glass after 400 days leaching at 90°C . Opaque particles are oxides of platinum group elements originally included in the glass sample. The position of original surface is indicated by the polished surface of the opaque particle located in the center of the figure.

of Na and Zn compared to the unaltered glass. The outermost portion of the altered layer is composed of a fibrous clay mineral (Fig. 8(b)). EDS analysis indicates that the clay mineral consists of mainly Si, Zn and Na.

The clay mineral on the altered glass surface was analyzed using XRD with thin film attachment. The XRD results show a 14 \AA reflection (Fig. 9(a)), which shifted to 17 \AA after ethylene glycol solvation (Fig. 9(b)). These results indicate that the clay mineral has a smectite-like structure.

SIMS profiles of H, B, Na, Cs, Cs and Si for the same sample are given in Fig. 10. The reciprocal depletion of

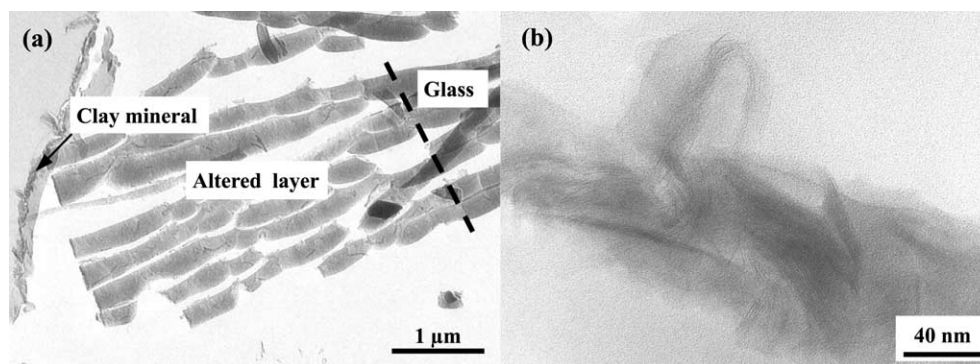


Fig. 8. TEM photomicrograph of P0798 glass after 400 days leaching at 90°C : (a) an entire view of the altered layer; (b) a higher magnification view of the clay mineral on the altered glass surface.

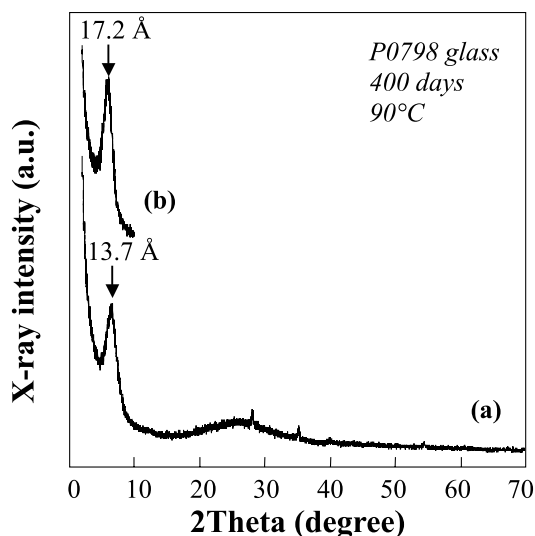


Fig. 9. XRD patterns of P0798 glass after 400 days leaching at 90°C: (a) air-dried sample; (b) ethylene glycol saturated sample. Two reflections around 30° are assigned to oxides of platinum group elements in glass.

B and Na as compared with an increase in H in the altered layer implies that the glass has undergone glass hydration. On the other hand, the lack of depletion of Si in the altered layer suggests that silica saturation in the solution prevents glass matrix dissolution. This agrees with the results of OM and TEM observation. The shapes of the elemental profiles are similar to those of the samples leached with amorphous silica powder (Figs.6(d) and (e)). This similarity implies that those samples were also altered by the same mechanism.

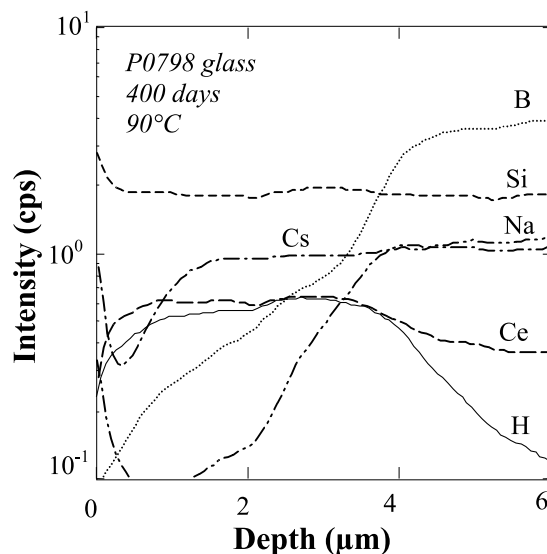


Fig. 10. SIMS depth profiles for P0798 glass after 400 days leaching at 90°C. (All profiles are normalized to that of the 'inert' element Al.)

Fig. 11 shows the thickness of the altered layer as a function of the square root of time. The thicknesses of altered layers in SIMS profiles of each sample were used for this plot. Those of the altered layer calculated based on the normalized elemental mass loss (NL) values for Na and B were also plotted in Fig. 11(a). The calculated thickness of the altered layer agrees well with the measured thickness. This agreement implies that the position of the glass surface has not changed, and is consistent with the OM observation described above. It is also

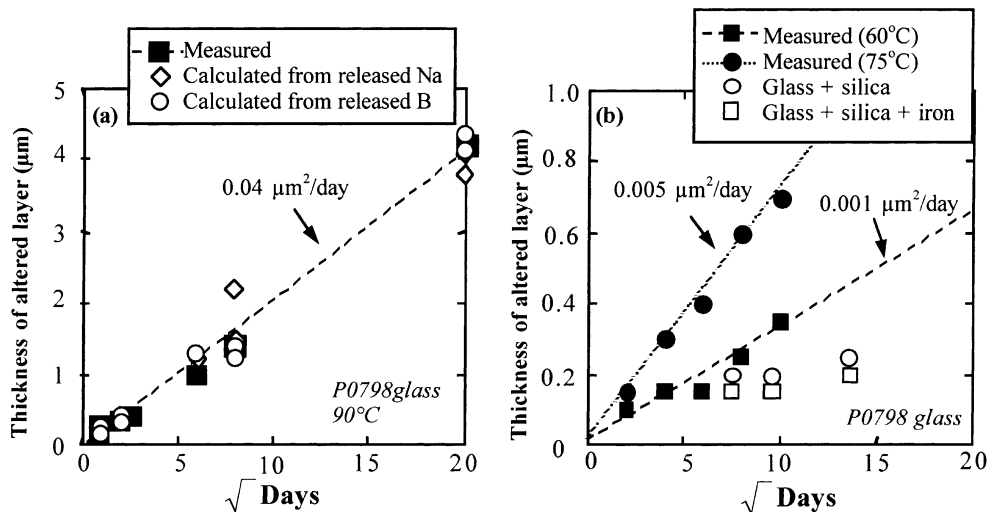


Fig. 11. Thickness of the altered layer versus the square root of time for P0798 glass leached in silica saturated solutions: (a) 90°C; (b) 60°C and 75°C. The results of integrated experiments with silica are also plotted in (b).

noted that the square root of time relationship for glass hydration is observed at the temperatures of 60°C, 75°C and 90°C. This relationship agrees with the results obtained from leaching experiments with powdered glasses [11–13]. Linear regression analyses of measured values resulted in glass hydration rates of 0.04, 0.005 and 0.001 $\mu\text{m}^2/\text{day}$ at 90°C, 75°C and 60°C, respectively. The measured altered layer thicknesses derived from the integrated experiments are slightly smaller than those of the sample leached by the MCC-1 type experiments (Fig. 11(b)). The reason of these differences might be related to solution pH.

The hydration rates were plotted versus temperature (expressed as $1000/T \text{ K}^{-1}$) in Fig. 12 together with those of high silica glasses ($\text{SiO}_2 > 70 \text{ wt}\%$), that were hydrated with deionized water [14–16]. The glass hydration rates of P0798 glass at each temperature are almost the same as for those glasses. The temperature dependence of hydration rates of P0798 glass can be expressed by the following Arrhenius equation:

$$k = 6.75 \times 10^{15} \exp(-120/RT), \quad (1)$$

where k is the hydration rate ($\mu\text{m}^2/\text{days}$), R the gas constant (8.3145 J/mol/K) and T is the temperature (K). The activation energy of 120 kJ/mol is higher than those for high silica glasses, which have undergone glass hydration. Furthermore, the activation energy of 120 kJ/mol is in fair agreement with that of Na diffusion in P0798 glass (113 kJ/mol for 155–300°C) [17]. This co-

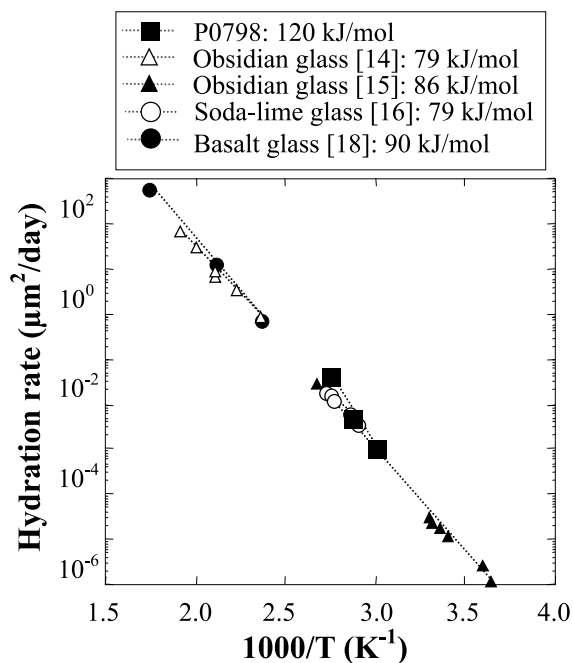


Fig. 12. Arrhenius diagram for hydration rates of various glasses.

incidence indicates that glass hydration, dominated by diffusion, is the alteration mechanism of waste glass under silica saturation conditions.

In Fig. 12, the hydration rates of basalt glass, which was hydrated with silica saturated solutions [18], were also plotted. Since Berger et al. [18] did not cite the hydration rates of basalt glass, we calculated the rates based on the square root of time relationship of their raw data. It is noted that the basalt glass has about the same temperature dependence of glass hydration, whereas the activation energy is slightly lower than that of P0798. These results imply that glass hydration is the principal alteration mode independent of glass composition under silica saturation conditions.

4. Conclusion

Leaching experiments in the presence of engineered barrier materials were performed with and without amorphous silica (integrated leaching experiments), to assess the effect of silica on the aqueous alteration of waste glass in contact with engineered barrier materials. The results of these experiments show the usefulness of a soluble silica additive for geological disposal of waste glass. The presence of amorphous silica effectively reduced the detrimental effects of the engineered barrier materials, because the concentration of silicic acid in the porewaters reaches the solubility of amorphous silica quickly.

MCC-1 type leaching experiments under silica saturation conditions demonstrate that the glass alteration under these conditions is dominated by glass hydration, and the release of soluble elements from waste glass closely follows a relationship dependent on the square root of time.

These studies imply that the prediction of long-term dissolution behavior of waste glass can be simplified by using a soluble siliceous material as an additional engineered barrier.

Acknowledgements

The authors gratefully acknowledge the invaluable assistance of M. Kubota of Inspection development corporation and enlightening comments from anonymous reviewers.

References

- [1] G.L. McVay, C.Q. Buckwalter, J. Am. Ceram. Soc. 66 (1983) 170.
- [2] J.W. Shade, L.R. Pederson, G.L. McVay, Adv. Ceram. 8 (1984) 358.

- [3] B.P. McGrail, *Nucl. Technol.* 75 (1986) 168.
- [4] T. Imakita, K. Sasakawa, F. Matsuda, R. Wada, *Mater. Res. Soc. Symp. Proc.* 333 (1994) 573.
- [5] Y. Inagaki, A. Ogara, H. Furuya, K. Idemitsu, *Mater. Res. Soc. Symp. Proc.* 412 (1996) 257.
- [6] N. Godon, E. Vernaz, J.H. Thomassin, J.C. Touray, *Mater. Res. Soc. Symp. Proc.* 127 (1989) 97.
- [7] N. Godon, Z. Andriambololona, E. Vernaz, *Mater. Res. Soc. Symp. Proc.* 257 (1992) 135.
- [8] Y. Minet, E. Vernaz, *Mater. Res. Soc. Symp. Proc.* 556 (1999) 633.
- [9] Y. Sasaki, M. Shibata, M. Yui, N. Sasaki, *Mater. Res. Soc. Symp. Proc.* 353 (1995) 337.
- [10] G.B. Mellinger, *Mater. Res. Soc. Symp. Proc.* 84 (1987) 483.
- [11] B. Grambow, W. Lutze, R. Müller, *Mater. Res. Soc. Symp. Proc.* 257 (1992) 143.
- [12] K. Lemmens, P. Van Iseghem, *Mater. Res. Soc. Symp. Proc.* 257 (1992) 49.
- [13] Y. Inagaki, H. Furuya, K. Idemitsu, S. Yonezawa, *J. Mater. Res.* 208 (1994) 27.
- [14] I. Friedman, R.L. Smith, W.D. Long, *Geol. Soc. Am. Bull.* 77 (1966) 323.
- [15] J.W. Michels, I.S.T. Tsong, G.A. Smith, *Archaeometry* 25 (1983) 107.
- [16] W.A. Lanford, K. Davis, P. Lamarche, T. Laursen, R. Groleau, R.H. Doremus, *J. Non-Cryst. Solids* 33 (1979) 249.
- [17] K. Nonaka, H. Nakajima, S. Mitsui, J. Echigoya, *J. Jpn. Inst. Met.* 64 (2000) 831, in Japanese.
- [18] G. Berger, C. Claparols, C. Guy, V. Daux, *Geochim. Cosmochim. Acta* 54 (1994) 4875.